Anion−Tri-s-triazine Bonding: A Case for Anion Recognition

Wenxu Zheng,[†] Ning-Bew Wong,*[,‡] and Anmin Tian*[,†]

Faculty of Chemistry, Sichuan University, Chengdu, Sichuan 610064, P R China, and Department of Biology and Chemistry, City University of Hong Kong, Kowloon, Hong Kong

Received: September 15, 2004; In Final Form: December 29, 2004

An ab initio study of the possible interaction between several anions (F^-, Cl^-, N_3^-, N_4^-, and N_5^-) and tri-s-triazine molecule, an electron-deficient aromatic ring, has been carried out at the B3LYP and MP2 levels of theory. Minima are located corresponding to hydrogen bonding, π-π stacking, and reactive complexes. This novel mode of bonding suggests the development of new cyclophane-type receptors for the recognition of anions.

Introduction

Cation recognition attracted considerable interest many years ago and is now a well-developed and mature area of supramolecular chemistry.[1] By contrast, the recognition and binding of anions received more attention only in recent years due to their important roles in the areas of biology, medicine, catalysis, and environment.[2] However, the design of anion receptors is particularly challenging. One reason is that anions are larger than isoelectrionic cations and therefore have a lower charge-to-radius ratio, which means the electrostatic binding interactions are less effective than they would be for the smaller cation. Another reason is that concentrations of positive potential are less accessible and manageable on the molecular scale than concentrations of negative potential, namely, localized electron deficits involved in Lewis acidic sites are inconveniently integrated into receptor design.

The types of noncovalent interaction used in anion recognition include electrostatic interactions, hydrogen bonding, hydrophobicity, coordination to a metal ion, and combinations of these interactions working together. In the previous work, many macrocyclic ammonium molecules were synthesized as anion receptors and were applied to both van der Waals interaction and hydrogen binding with halides and various oxyanions.[3−7] Although several such macrocycles are cyclophanes, in no case does the aromatic π-system participate in the coordination. Generally, the aromatic rings are regarded as sources of electron density and are thus respected to interact repulsively with anions. However, Mascal and co-workers have recently reported the interaction between s-triazine and the fluoride, chloride, and azide ion.[8] This is the first theoretical demonstration of an interaction between a formally negatively charged species and the π-system of an aromatic ring. Our interest in the properties of tri-s-triazine molecule[9,10] led us to consider whether it could also interact with these anions and whether the interaction intensity could exceed that of s-triazine.

Methods

The local minima of the supramolecular complexes were fully optimized by analytic gradient techniques. The methods used were the density functional theory (DFT) with Becke's three-parameter (B3)[11] exchange functional along with the Lee−Yang−Parr (LYP) nonlocal correlation functional (B3LYP)[12,13] and the second-order Møller−Plesset perturbation (MP2) theory. The standard valence double-ζ basis set augmented with d-type polarization functions and s- and p-type diffuse functions, 6-31+G (d),[14] was used. In the B3LYP/6-31+G (d) level calculations of harmonic vibrational frequency, the force constants were determined analytically for all of the supermolecules. Basis set superposition error (BSSE) was corrected for all calculations by applying Boys and Bernardi's counterpoise procedure (CP).[15] The Gaussian 98 program was used in the calculations.[16]

To analyze the bonding characteristics of supramolecular complexes, the atoms in molecules (AIM) theory of Bader[17] was applied with the AIM 2000 program package.[18] The AIM theory is based on a topological analysis of the electron charge density and its Laplacian. This theory has proved itself a valuable tool to conceptually define what is an atom and, above all, what is a bond in a quantum calculation of a molecular structure. The analysis went further with those obtained by means of the natural bond orbital (NBO) theory of Weinhold and co-workers.[19] This analysis allows us to isolate the interaction energies in low-order perturbative expressions of easily interpretable form and to relate these expressions to chemical explanations. The bond interaction in the various supermolecules is discussed in terms of stabilization energies, $\Delta E_{(2)}$, which is calculated by the second-order perturbation analysis of the Fock matrix obtained in the NBO analysis. By this perturbational approach, the donor−acceptor interaction involving a filled orbital σ (donor) and an unfilled antibonding orbital φ^* (acceptor) can be quantitatively described. Specifically, this stabilization energy is calculated by the following expression:

$$\Delta_\sigma \varphi^* E_{(2)} = -2\frac{(\langle\sigma|F|\varphi^*\rangle)^2}{\epsilon_{\varphi}{}^* - \epsilon_\sigma}$$

where F is the Fock operator and ϵ_σ and ϵ_{φ^*} are the NBO energies of the donor and acceptor orbitals, respectively.

Molecular electrostatic potentials (MEPs)[20−22] are utilized to probe molecular structure and reactivity. The topographical properties of MEP were effectively used by Gadre and co-

* Corresponding authors. E-mail Addresses: Anmin Tian <suqcp@mail.sc.cninfo.net>; Ning-Bew Wong <bhnbwong@cityu.edu.hk>.
† Sichuan University.
‡ City University of Hong Kong.

10.1021/jp045827k CCC: $30.25
Published on Web 02/08/2005

workers.[23,24] The rigorous topographical parameters, namely, the critical points (CPs) of the MEP distribution, represent structural as well as reactivity indices of the molecule as has been demonstrated by Gadre et al.[25] MEP topographical parameters were obtained in terms of the CPs of the MEP distribution. The CPs are the points at which the gradient of the scalar field vanishes, i.e., $\nabla V(r) = 0$. The CPs are further characterized from the eigenvalues of the Hessian matrix. A simple notation for the description of CPs is in terms of (R, s), with R being the rank of the Hessian matrix and s is the signature (which is simply algebraic sum of the sign of the eigenvalues). Thus, there are four types of nondegenerate CPs: (3, +3) minimum, (3, −3) maximum, and (3, +1) and (3, −1) saddles. The amount of eigenvalues at the CP indicates the relative change of function in a direction. The MEPs of s-triazine, tri-s-triazine, and anions concerned in this paper were calculated at MP2/6-31+G (d) level at the optimized geometries with Gaussian98, and the 3D contour maps were plotted using gOpenMol 2.32.[26,27]

Results and Discussion

Gadre et al. had studied the molecular electrostatic potential (MEP) maps of some anions containing N_3^-.[28,29] To gain insight into the electron distribution of the anions concerned in this study, we first investigated the MEPs of N_3^-, $N4^-$, and $N5^-$ anions in details. Figure 1 displays the MEP contour maps of these anions in the molecular plane containing the molecular axis. There is a positive valued saddle point (denoted by a solid circle) between two adjacent nitrogen nuclei in each anion. Furthermore, there exist four minima (shown by plus) and four negative valued saddle points (shown by asterisk) for N_3^- and $N4^-$ anions. As for $N5^-$ anion, five minima and five negative valued saddle points can be found. Starting from any nucleus in the outward direction, there always exists a directional minimum. The minimum valued contour engulfing all the nuclei of the anion has value −0.18 au for N_3^-, −0.18 au for N_4^-, and −0.20 au for N_5^-. The distance between the negative valued saddle points along the molecular axis is 5.035 Å, and the distance between the negative valued saddle points along axis perpendicular to molecular axis is 3.664 Å for N_3^-. These distances suggest that the radius of N_3^- anion should be within the range of 1.8 ∼ 2.5 Å. N_4^- and N_5^- anions have a planar cyclic structure. The distances from the negative valued critical points to the center of the ring amount to 2.384 and 2.520 Å for N_4^- and 2.116, 2.424, and 1.855 Å for N_5^-. As predicted in the above cases, the radius of N_4^- should not be less than 2.384 Å and not exceed 2.520 Å, and the radius of N_5^- should be greater than 1.855 Å and less than 2.424 Å.

Mascal et al. investigated the interaction between s-triazine and the fluoride, chloride, and azide anions at the MP2 level of theory.[8] In the present work, MP2 failed to locate some minima confirmed with DFT, and we therefore considered both MP2 and B3LYP in our study.

Hydrogen Bonding Complexes. Figure 2 illustrates the initial H-bonding supramolecular structures 1A−5A$_V$. The subscript P denotes a planar complex, and V, a nonplanar one. All the local minima of these supermolecules are depicted in Figure 3. It should be noticed that local minima of 4A$_P$ and 4A$_V$ with N_4^- anion could not be obtained with MP2 method, and 5A$_P$ with N_5^- anion could not be obtained with either MP2 or B3LYP methods.

These H-bonds are of good quality, as judged by the short H···X (X=F, Cl, N) distances (about 1.4∼2.2 Å) and C−H···X angles at 180°. Since all of the calculations are

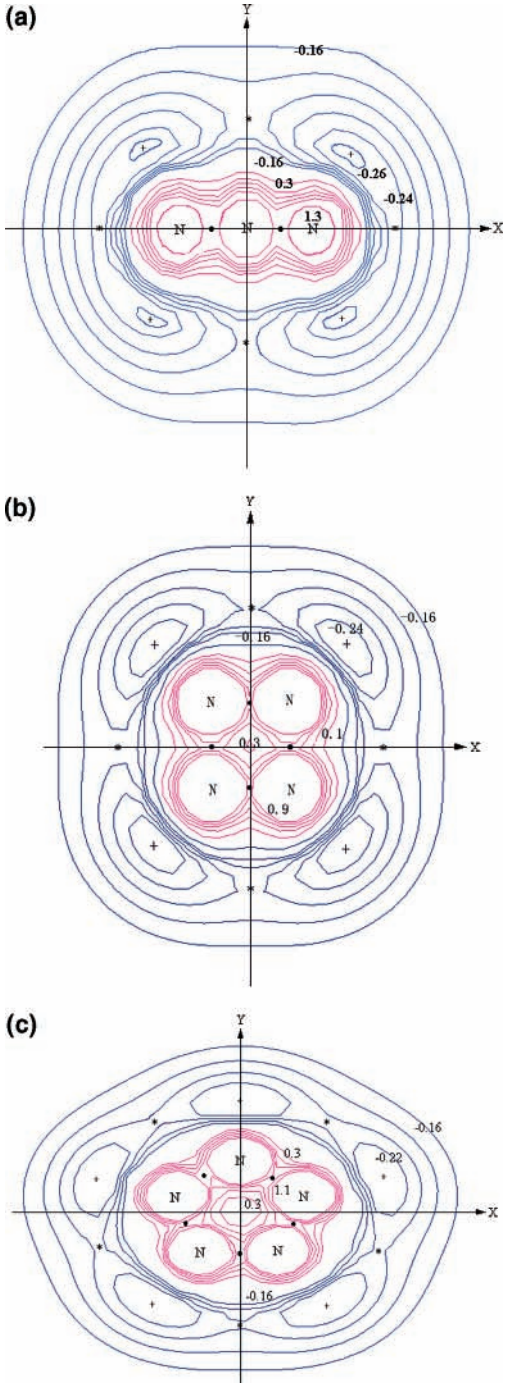

Figure 1. Molecular electrostatic potential of N_3^-, $N4^-$, and $N5^-$ anions in the plane containing the molecular axis. The red line represents the positive part of the electrostatic potential, and the blue line represents the negative part of the electrostatic potential. The contour spacing is 0.02 au for the negative part and 0.2 au for the positive part. All the units are in a.u. (a) The nitrogens are at (2.308, 0.0, 0.0), (0.0, 0.0, 0.0), and (−2.308, 0.0, 0.0). The coordinates and MEP at the critical points are ● (1.399, 0.0, 0.0) 1.10; * (4.757, 0.0, 0.0) −0.15 and (0.0, 3.462, 0.0) −0.19; + (3.231, 2.423, 0.0) −0.27. (b) The nitrogens are at (1.266, −1.387, 0.0), (1.266, 1.387, 0.0), (−1.266, 1.387, 0.0) and (−1.266, −1.387, 0.0). The coordinates and MEP at the critical points are ● (1.287, 0.0, 0.0) 0.60 and (0.0, 1.383, 0.0) 0.80; * (4.505, 0.0, 0.0) −0.19 and (0.0, 4.762, 0.0) −0.19; + (3.218, 3.475, 0.0) −0.25. (c) The nitrogens are at (2.056, 0.668, 0.0), (0.0, 2.161, 0.0), (1.270, −1.748, 0.0), (−2.056, 0.668, 0.0) and (−1.270, −1.748, 0.0). The coordinates and MEP at the critical points are ● (1.00, 1.375, 0.0) 0.80, (1.618, −0.525, 0.0) 0.80, and (0.0, −1.700, 0.0) 0.80; * (2.740, 2.912, 0.0) −0.21, (4.421, −1.201, 0.0) −0.21, and (0.0, −3.505, 0.0) −0.21; + (4.501, 1.256, 0.0) −0.23, (2.720, −3.020, 0.0) −0.23, and (0.0, 3.595, 0.0) −0.23.

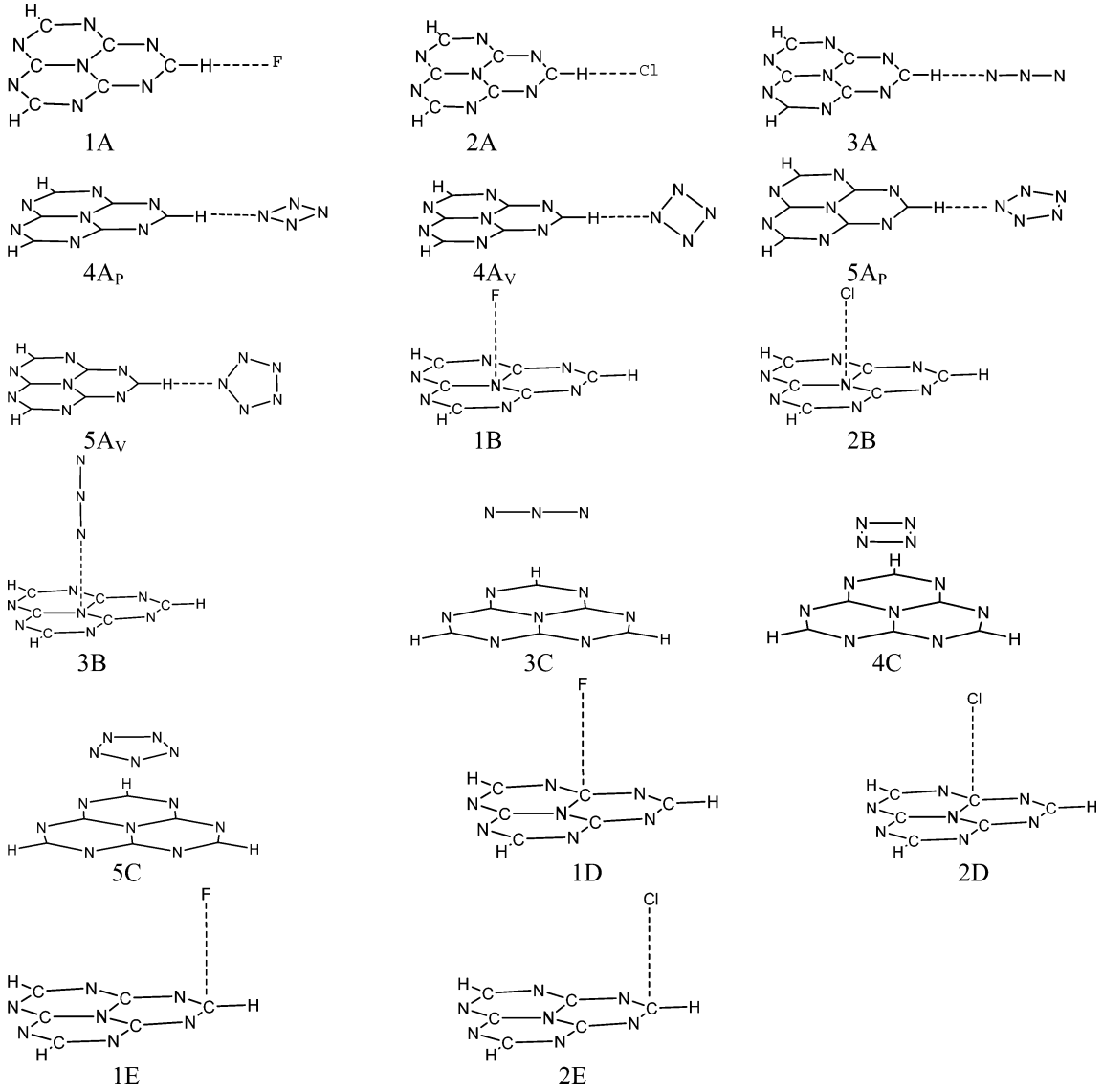

Figure 2. Initial structures of anion−tri-s-triazine supermolecules.

TABLE 1: MP2/6-31+G(d) and B3LYP/6-31+G(d) Binding Energies (kcal mol^{-1}) for Complexes of Tri-s-triazine and Anions

	ΔE_{MP2}	$\Delta E_{MP2-BSSE}$	ΔE_{B3LYP}	$\Delta E_{B3LYP-BSSE}$
1A	−28.93	−26.54	−30.69	−29.37
1B	−36.21	−31.69	−31.69	−29.81
1D	−88.67	−80.26	−84.78	−82.08
1E	−86.72	−79.51	−83.58	−81.20
2A	−15.31	−12.24	−12.99	−12.86
2B	−27.48	−20.52	−17.45	−17.13
2D	−54.28	−41.85	−40.98	−40.29
2E	−56.10	−45.37	−23.59	−23.22
3A	−13.68	−11.73	−13.93	−13.49
3B	−26.42	−21.34	−18.45	−17.38
3C	−28.55	−21.02	−16.51	−15.25
4A$_P$			−10.17	−9.98
4A$_V$			−10.92	−10.54
4C	−28.05	−18.83	−13.43	−11.80
5A$_V$	−11.73	−9.48	−9.54	−9.22

performed at the same level of theory with ref 8, the slightly shorter H-bond distances of our results suggest that the H-bond strengths of tri-s-triazine-anion complexes are little stronger than those of s-triazine-anion complexes. This result can be confirmed by checking binding energies listed in Table 1. The counterpoise corrected MP2 binding energies for fluoride−tri-s-triazine(1A), chloride−tri-s-triazine(2A), azide−tri-s-triazine(3A), and N_5^- −tri-s-triazine(5A$_V$) complexes have been evaluated to be −26.54 kcal mol^{-1}, −12.24 kcal mol^{-1}, −11.73 kcal mol^{-1}, and −9.48 kcal mol^{-1}, respectively. The corresponding B3LYP values are very close to MP2 results. For N_4^- −tri-s-triazine complexes, we can get two local minima 4A$_P$ and 4A$_V$ only at the B3LYP level. The H···N distance in planar complex 4A$_P$ amounts to 2.143 Å, about 0.08 Å larger than that in nonplanar complex 4A$_V$, and corresponding binding energy for former is smaller than that for latter. For the N_5^- −tri-s-triazine complex, only nonplanar local minimum 5A$_V$ can be obtained. These results indicate that when N_4^- and N_5^- anions attack the hydrogen atom of tri-s-triazine molecule, a nonplanar hydrogen bonding complex forms more easily than does a planar one.

The rigorous AIM theory[17] has been successfully applied in interpretation of charge density concerning a wide variety of chemical systems.[30,31] Popelier proposed a set of criteria for the existence of H bonding within the AIM formalism.[32,33] The most prominent evidence of hydrogen bonding is the existence of a bond path between the donor hydrogen nucleus and the acceptor, and a bond critical point (BCP) at which the electron density (ρ_b) ranges from 0.002 to 0.035 au and the Laplacian of the electron density ($\nabla^2\rho_b$) ranges from 0.024 to 0.139 au. The five other criteria deal with changes of atomic charge q(H), atomic polarization moment M(H), atomic volume v(H), atomic

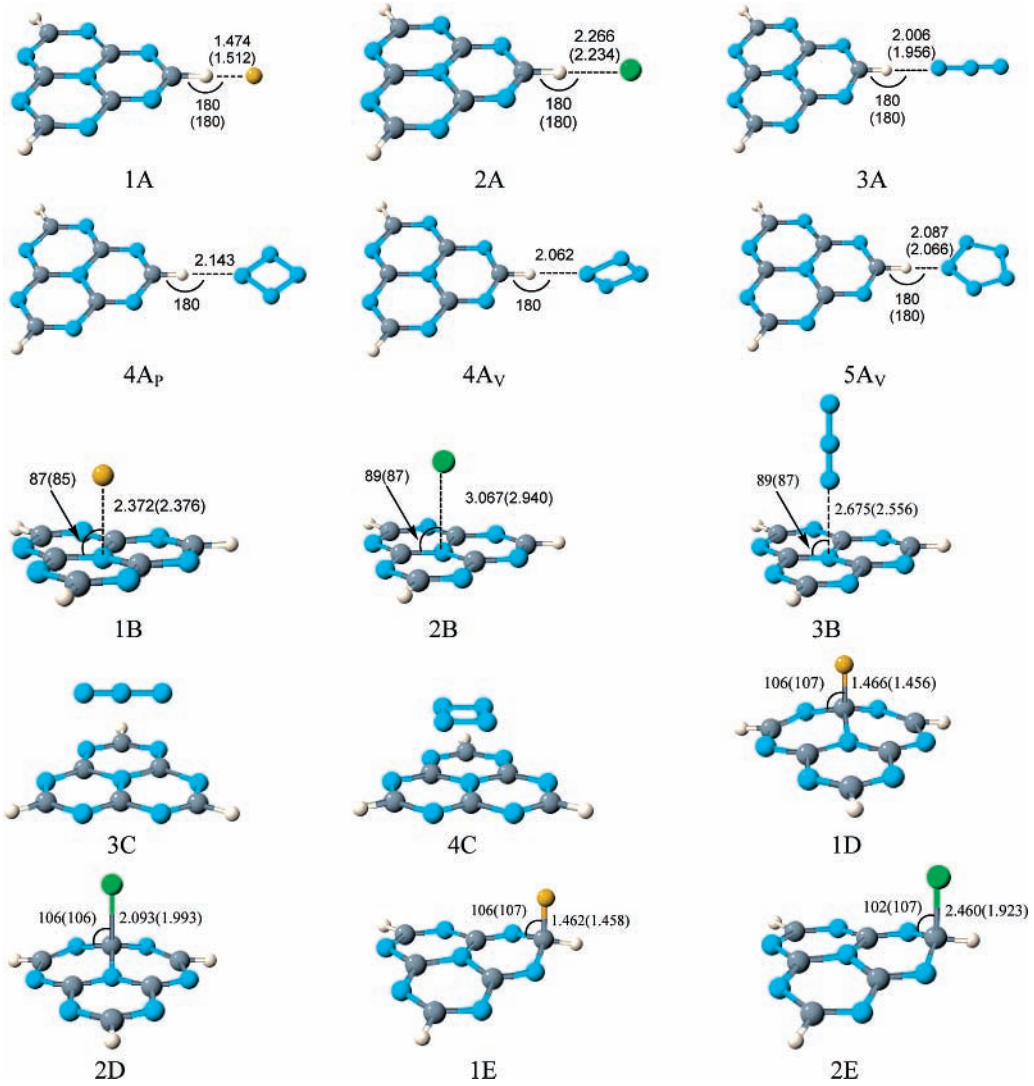

Figure 3. Optimized structures of anion−tri-s-triazine supermolecules along with selected bond lengths (in Å) and bond angles (in °) at B3LYP/6-31+g (d) level of theory. MP2/6-31+g (d) results listed in parentheses.

TABLE 2: Charge Density (ρ_b) and Its Laplacian ($\nabla^2\rho_b$) at BCPs between Anions and Tri-s-triazine at B3LYP/6-31+G(d) Level of Theory (a.u.)

	1A	2A	3A	4A$_P$	4A$_V$	5A$_V$	1D	2D	1E	2E
ρ_b	0.075	0.024	0.024	0.021	0.025	0.024	0.202	0.119	0.205	0.135
$\nabla^2\rho_b$	0.236	0.064	0.084	0.060	0.068	0.068	−0.156	−0.060	−0.240	−0.112

energy E(H), and atomic radius r(H) of the hydrogen atom upon formation of the hydrogen bond. The AIM calculations in the present study were performed at the B3LYP/6-31+G (d) level of theory. The charge densities of the BCPs are listed in Table 2. The large value (0.075) of the density at the BCP of the H···F bond coincides with its short bond length in 1A, and other values all fall in the range considered by the criterion of the H-bond. According to Table 2, all the $\nabla^2\rho_b$ are positive, which confirms their H-bonding property. Another important criterion of hydrogen bond formation is based on the mutual penetration of the hydrogen (H) and acceptor atom (A). The penetration is defined as the nonbonded radius minus the bonded radius. According to Table 3, the acceptor atom is penetrated more than the hydrogen atom. Again, the strongest mutual penetration occurs in the fluoride−tri-s-triazine (1A) complex. Upon dimerization, the net charges of the donor hydrogen atoms all increase, as illustrated by Table 3. From this table, we can also see that the energies of all hydrogen atoms are augmented, which means that the hydrogen atom is destabilized in the complex.

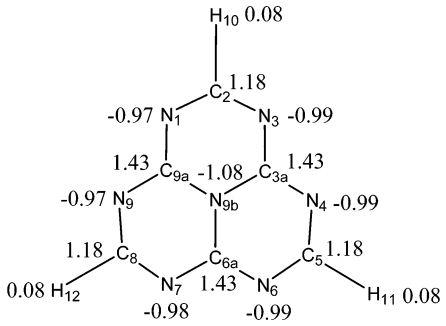

Figure 4. AIM atomic charges for tri-s-triazine (the integration radius is 0.5 au for all the atoms).

Table 3 also shows that the magnitude of the dipolar polarization (M_H) of the hydrogen atomic distribution is decreasing upon complex formation, and this is primarily a result of the loss of the nonbonded density of the hydrogen atom. In view of the hydrogen atom's volume given in Table 3, all the quantities

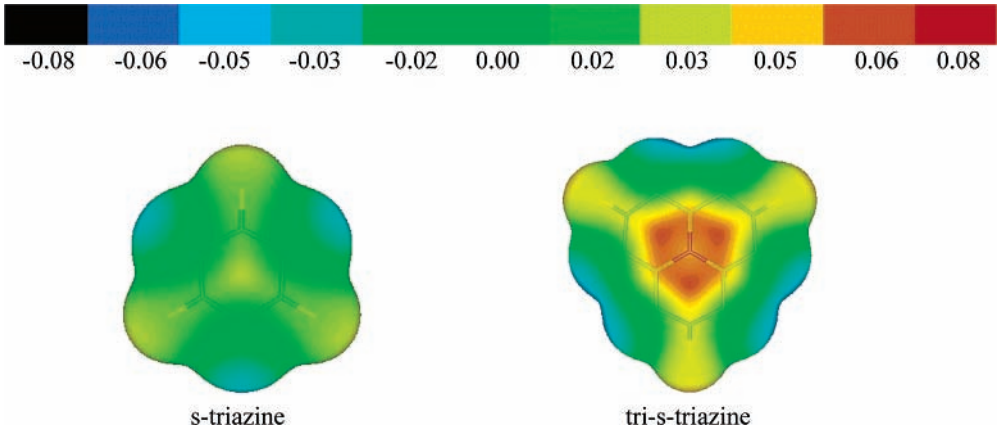

Figure 5. Calculated MP2/6-31+G (d) electrostatic potential textured vdW surfaces for s-triazine and tri-s-triazine molecules.

TABLE 3: H Atomic Basin Integrated Properties and H and A (F^-, Cl^- or N) Bond Radii in the H-bond Complex (unit: a.u.)

	q_H	Δq_H	M_H	ΔM_H	υ_H	$\Delta\upsilon_H$	E_H	ΔE_H	r_H	Δr_H	r_A	Δr_A
1A	0.4232	−0.3123	0.0586	0.0885	19.044	24.021	−0.4202	−0.1621	0.9061	1.5399	1.8786	1.7214
2A	0.2672	−0.1563	0.1294	0.0177	32.582	10.483	−0.4959	−0.0864	1.4484	0.9976	2.8329	1.5171
3A	0.2609	−0.1500	0.1141	0.0330	31.044	12.021	−0.5124	−0.0699	1.4171	1.0289	2.3739	1.2261
$4A_P$	0.2584	−0.1475	0.1334	0.0137	32.583	10.482	−0.5101	−0.0722	1.4971	0.9489	2.5518	1.2901
$4A_V$	0.2794	−0.1685	0.1252	0.0219	30.754	12.311	−0.4983	−0.0840	1.4164	1.0296	2.4796	1.3623
$5A_V$	0.2666	−0.1557	0.1198	0.0273	31.055	12.010	−0.5070	−0.0753	1.4353	1.0107	2.5077	1.2923

TABLE 4: Stabilization Interaction Energies $E_{(2)}$ (kcal mol^{-1}) at B3LYP/6-31+G (d) Level for Hydrogen Bonding Complexes

	donor NBOs	acceptor NBOs	$\Delta E_{(2)}$
1A	F lone pair	C−H antibond	60.03
2A	Cl lone pair	C−H antibond	17.95
3A	N lone pair	C−H antibond	13.94
$4A_P$	N lone pair	C−H antibond	5.05
$4A_V$	N lone pair	C−H antibond	6.67
$5A_V$	N lone pair	C−H antibond	12.85

are decreasing for all the hydrogen atoms. In general, the degree of hydrogen atom shrinking is in proportion to the strength of the hydrogen bond.

Formation of a H-bonding complex involves CT from the proton acceptor to the proton donor. This results in the increase of charge density in the X−H antibonding orbitals of the proton donor. Since the charge transfer accompanies the formation of hydrogen bonds and plays a major role in it, $\Delta E_{(2)}$ can be taken as an index to judge the strength of hydrogen bonds. To obtain $\Delta E_{(2)}$, we performed NBO analysis at the B3LYP/6-31+G (d) level. The calculated results listed in Table 4 suggest that the stabilization energy terms completely come from lone-pair − empty-orbital interaction. The value of $\Delta E_{(2)}$ for fluoride−tri-s-triazine (1A) complex is outstanding, which is in accordance with the order of binding energy, suggesting that the CT is an important factor in these intermolecular interactions.

From the above discussion, we can confirm that these H-bonds are of good quality.

Electrostatic Complexes. The AIM atomic charges of tri-s-triazine are illustrated in Figure 4. Although the net charge for central nitrogen (N_{9b}) of tri-s-triazine ring is negative, the 3D MEP map of tri-s-triazine (Figure 5) clearly indicates an area of positive charge concentrated on the center of the ring. Moreover, checking the 2D MEP maps of tri-s-triazine on the molecular plane (Figure 6) and 1.5 Å above the molecular plane (Figure 7), the results are similar to that of 3D map. Therefore, from the viewpoint of electrostatic interactions, this molecule is expected to form electrostatic complexes with anions. This type of interaction contains complexes 1B−3B, 3C and 4C illustrated in Figure 2. With regard to 1B−3B, the local minima

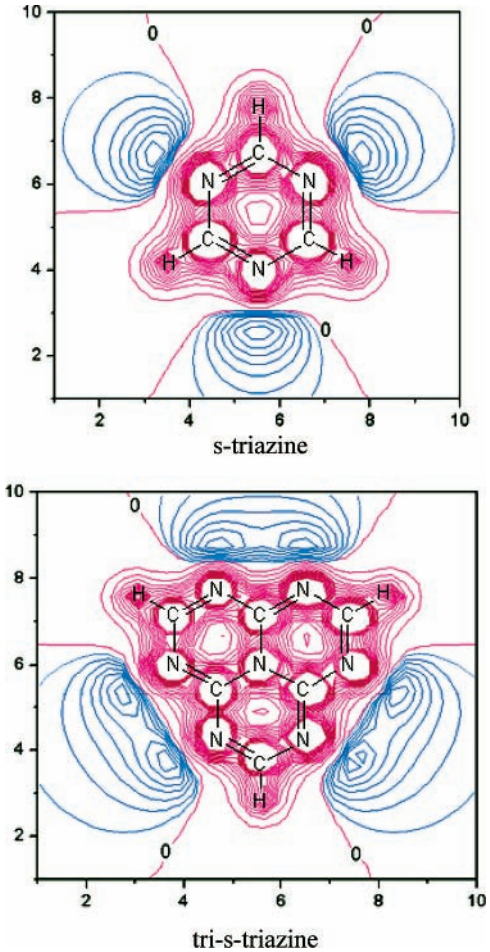

Figure 6. Electrostatic potential maps of s-triazine and tri-s-triazine on the molecular plane. The red line represents the positive part of the electrostatic potential, and the blue line represents the negative part of the electrostatic potential. The contour spacing is 0.1 au for the positive part and 0.01 au for the negative part. The unit of the axes is angstroms.

of them can be obtained with both B3LYP and MP2 methods. The counterpoise corrected MP2 binding energies are −31.69

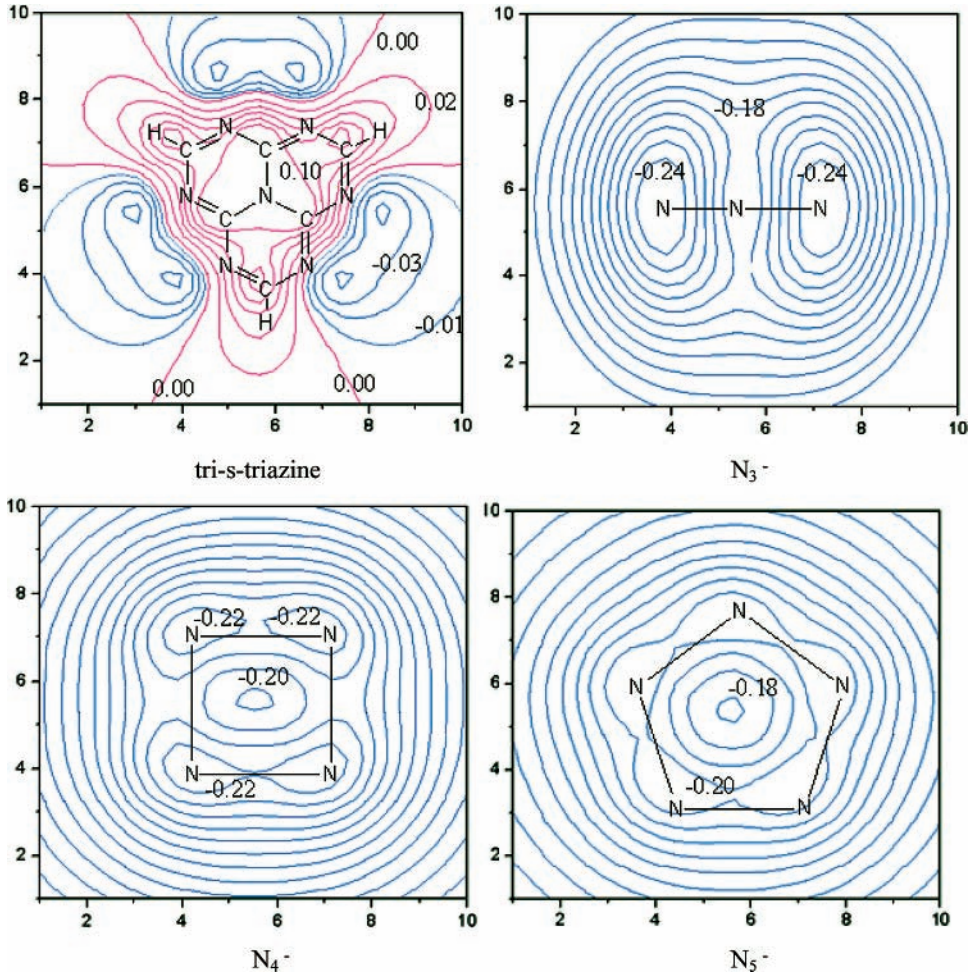

Figure 7. Electrostatic potential maps of tri-s-triazine, N_3^-, N_4^-, and N_5^- on the 1.5 Å above molecular plane. The red line represents the positive part of the electrostatic potential, and the blue line represents the negative part of the electrostatic potential. The contour spacing is 0.02 au for the positive part and 0.01 au for the negative part. The unit of the axes is angstroms.

kcal mol^{-1} for 1B, −20.52 kcal mol^{-1} for 2B, and −21.34 kcal mol^{-1} for 3B, respectively, much stronger than corresponding H-bonding complexes. As shown in Figure 3, the anions locate on the C_3 axis of the tri-s-triazine molecule, which is as anticipated from electrostatic augments. B3LYP results indicate that the distances between anions and central nitrogen of tri-s-triazine are 2.372 Å for 1B, 3.067 Å for 2B, and 2.675 Å for 3B, respectively. These amounts are very close to those of MP2 results.

The N_3^- and N_4^- anions were found to participate in an apparent π-π staking interaction with tri-s-triazine, i.e., 3C and 4C (Figure 3). B3LYP and MP2 calculations both predict that the mean interplanar distance is about 2.7 Å for 3C and 2.8 Å for 4C. The close approach of the two fragments is consistent with the substantial binding energy calculated for 3C and 4C (Table 1). Efforts to find an analogous minimum for N_5^-−tri-s-triazine were not successful. We calculated the MEP of N_3^-, N_4^-, and N_5^- anions; the 2D counter maps of them are depicted in Figure 7. From the MEP map above 1.5 Å molecular plane, it is clear that the negative MEP displays successively smaller value in the order N_3^-, N_4^-, and N_5^-. The MEP of N_5^- is too small to form a π-π staking complex with tri-s-triazine.

***σ*-Complexes.** When F^- and Cl^- anions attack the carbon atoms of a tri-s-triazine molecule, four minima (1D, 1E, 2D, and 2E, Figure 3) can be obtained with both B3LYP and MP2 methods. These new minima are suggestive of reactant complexes. The MP2 predicted anion−carbon distances of approximately 1.456 Å for 1D, 1.458 Å for 1E, 1.993 Å for 2D, and 1.923 Å for 2E, only slightly longer than the typical $C_{sp}3$−F and $C_{sp}3$−Cl bonds. Due to the strong interactions, tri-s-triazine molecule has lost its plane geometry in these complexes. As expected, the counterpoise corrected MP2 binding energies for 1D, 1E, 2D, 2E were evaluated to be −80.26, −79.51, −41.85, and −45.37 kcal mol^{-1}, respectively. These values are much larger than those for the corresponding H-bonding and electrostatic complexes.

Regarding these σ-complexes, it is important to analyze the local properties of anion−carbon bonds. Table 2 lists the electron density (ρ_b) and its Laplacian ($\nabla^2\rho_b$) at the BCPs of anion−carbon bonds. The general features of these magnitudes are common of covalent bonds, i.e., ρ_b values about 0.1−0.2 au, negative values of $\nabla^2\rho_b$ indicative of local concentration of charge at the bond. It has been shown that ρ_b is related to the bond order and thus to the bond strength. As a result, the value for ρ_b is much higher for F−C bond compared to the Cl−C bond. Natural bond orbital (NBO) analysis indicates that these anion−carbon bonds are composed of P_Z orbital of F, Cl, and C atoms, and the Wiberg bond indexes are about 0.7 for the F−C bond and 0.6 for the Cl−C bond.

Conclusion

In summary, we have systematically described the results of quantum chemical calculations (MP2 (B3LYP)/6-31+G (d) level) on the intermolecular interaction of tri-s-triazine molecule with several anions. The geometry, energy, and electron density

properties of these hydrogen bonding, electrostatic and reactant complexes have been studied. The calculations have shown that all the complexes studied are local minima of the potential energy surface. The binding energies for these interactions range from −9 to −80 kcal mol^{-1}. Our calculation results suggest that the tri-s-triazine ring should be applicable as a new anion recognition module in cyclophane chemistry and as a depot forming adjuvant for nitrogen clusters, such as N_3^-, N_4^-, and N_5^-.

Acknowledgment. This work was supported by the Research Grants Council of Hong Kong (Project No. 9040979 (CityU 102404)), the National Science Foundation of China (20373045) and Special Research Foundation of Doctoral Education of Chinese University (20020610024). The authors wish to thank Prof. Jiande Gu for useful suggestions.

References and Notes

(1) Beer, P. D.; Gale, P. A. *Angew. Chem., Int. Ed.* **2001**, *40*, 486.
(2) *Supramolecular Chemistry of Anions*; Bianchi, A.; Bowman-James, K.; Garcia-Espana, E., Eds.; Wiley−VCH: New York, 1997.
(3) Park, C. H.; Simmons, H. E. *J. Am. Chem. Soc.* **1968**, *90*, 2431.
(4) Schmidtchen, F. P. *Angew. Chem.* **1977**, *89*, 751.
(5) Schmidtchen, F. P. *Chem. Ber.* **1980**, *113*, 864.
(6) Hosseini, M. W.; Lehn, J.-M. *J. Am. Chem. Soc.* **1982**, *104*, 3525.
(7) Hosseini, M. W.; Lehn, J.-M. *Helv. Chim. Acta* **1986**, *69*, 587.
(8) Mascal, M.; Armstrong, A.; Bartberger, M. D. *J. Am. Chem. Soc.* **2002**, *124*, 6274.
(9) Zheng, W. X.; Wong, N. B.; Wang, W. Z.; Zhou, G.; Tian, A. M. *J. Phys. Chem. A*, **2004**, 108, 97.
(10) Zheng, W. X.; Wong, N. B.; Liang, X. Q.; Long, X. P.; Tian, A. M. *J. Phys. Chem. A* **2004**, *108*, 97.
(11) Becke, A. D. *J. Chem. Phys.* **1993**, *98*, 5648.
(12) Lee, C.; Yang W.; Parr, R. G. *Phys. Rev. B* **1988**, *37*, 785−789.
(13) Miehlich, B.; Savin, A.; Stoll H.; Preuss, H. *Chem. Phys. Lett.* **1989**, *157*, 200.
(14) Hehre, W. J.; Radom, L.; Schleyer, P. v. R.; Pople, J. A. *Ab Initio Molecular Orbital Theory*; Wiley: New York, 1986.
(15) Boys, S. F.; Bernardi, F. *Mol. Phys.* **1970**, *19*, 553.
(16) Frisch, M. J.; Trucks, G. W.; Schlegel, H. B.; Scuseria, G. E.; Robb, M. A.; Cheeseman, J. R.; Zakrzewski, V. G.; Montgomery, J. A., Jr.; Stratmann, R. E.; Burant, J. C.; Dapprich, S.; Millam, J. M.; Daniels, A. D.; Kudin, K. N.; Strain, M. C.; Farkas, O.; Tomasi, J.; Barone, V.; Cossi, M.; Cammi, R.; Mennucci, B.; Pomelli, C.; Adamo, C.; Clifford, S.; Ochterski, J.; Petersson, G. A.; Ayala, P. Y.; Cui, Q.; Morokuma, K.; Malick, D. K.; Rabuck, A. D.; Raghavachari, K.; Foresman, J. B.; Cioslowski, J.; Ortiz, J. V.; Stefanov, B. B.; Liu, G.; Liashenko, A.; Piskorz, P.; Komaromi, I.; Gomperts, R.; Martin, R. L.; Fox, D. J.; Keith, T.; Al-Laham, M. A.; Peng, C. Y.; Nanayakkara, A.; Gonzalez, C.; Challacombe, M.; Gill, P. m. W.; Johnson, B.; Chen, W.; Wong, M. W.; Andres, J. L.; Gonzalez, C.; Head-Gordon, M.; Replogle, E. S.; Pople, J. A. *Gaussian 98*, Revision A.11; Gaussian, Inc.: Pittsburgh, PA, 2001.
(17) Bader, R. F. W. *Atoms in Molecules, A Quantum Theory*; Oxford University Press: Oxford, 1990.
(18) Biegler-König, F.; Schönbohm, J.; Derdau, R.; Bayles, D.; Bader, R. F. W. *AIM 2000*, Version 2.0; McMaster University, 2002.
(19) (a) Reed, A. E.; Weinstock, R. B.; Weinhold, F. *J. Chem. Phys.* **1985**, *83*, 735. (b) Reed, A. E.; Weinstock, R. B.; Weinhold, F. *J. Chem. Phys.* **1985**, *83*, 1736. (c) Reed, A. E.; Curitss, L. A.; Weinhold, F. *Chem. Rev.* **1988**, *88*, 899.
(20) Politzer, P. Murray, J. S. In *Molecular Electrostatic Potentials: Concepts and Applications*; Murray, J. S., Sen, K. D., Eds.; Elsevier: Amsterdam, 1996; p 649.
(21) Boris, B.; Petia, B. *J. Phys. Chem. A* **1999**, *103*, 6793.
(22) Gadre, S. R.; Bhadane, P. K. *J. Phys. Chem. A* **1999**, *103*, 3512.
(23) Gadre, S. R.; Kulkarni, S. A.; Shrivastava, I. H. *J. Chem. Phys.* **1992**, *96*, 5253.
(24) Shirsat, R. N.; Bapat, S. V.; Gadre, S. R. *Chem. Phys. Lett.* **1992**, *200*, 373.
(25) Mehta, G.; Gunasekaran, G.; Gadre, S. R.; Shirsat, R. N. Ganguly, B.; Chandrasekhar, J. *J. Org. Chem.* **1994**, *59*, 1953.
(26) Laaksonen, L. *J. Mol. Graph.* **1992**, *10*, 33.
(27) Bergman, D. L.; Laaksonen, L.; Laaksonen, A. *J. Mol. Graph. Model.* **1997**, *15*, 301.
(28) Gadre, S. R.; Shrivastava, I. H. *J. Chem. Phys.* **1991**, *94*, 4384.
(29) Gadre, S. R.; Kölmel, C.; Shrivastava, I. H. *Inorg. Chem.* **1992**, *31*, 2279.
(30) Louit, G.; Hoquet, A.; Ghomi, M.; Meyer, M.; Sühnel J. *PhysChemComm* **2003**, *6*, 1.
(31) Louit, G.; Hoquet, A.; Ghomi, M.; Meyer, M.; Sühnel, J. *PhysChemComm* **2002**, *5*, 94.
(32) Koch, U.; Popelier, P. L. A. *J. Phys. Chem.* **1995**, *99*, 9747.
(33) Popelier, P. L. A. *J. Phys. Chem. A* **1998**, *102*, 1873.